

SUPPORTING INFORMATION

Charge transport control via polymer polymorph modulation in ternary organic photovoltaic composites

Zhipeng Kan ^a, Letizia Colella ^{b, c}, Eleonora Canesi ^{a, b}, Alexei Vorobiev ^{d, e}, Vasyl Skrypnichuk ^f, Giancarlo Terraneo ^{a, b}, David R. Barbero ^f, Chiara Bertarelli ^{a, b}, Roderick C. I. Mackenzie ^g, Panagiotis E. Keivanidis ^h

Two-dimensional Grazing Incidence Wide Angle X-ray Scattering (2D-GIWAXS) measurements

Data Acquisition: The two-dimensional GIWAXS data was collected at the beamline BM26 of the European Synchrotron Radiation Facility (ESRF, Grenoble, France). The acquisition was carried out using Frelon CCD camera (pixel size 0.0468×0.0468 mm, matrix size 2048×2048 pixels; sample-detector distance 204.3691 mm, wavelength 1.24 Å, horizontal sample orientation; beam location: 1010.745 (horizontal), 217.6495 (vertical). Every sample was measured at angle of 0.3 deg. For this angle three images were collected and then averaged by the data reduction script provided by BM26.

GIWAXS data analysis: The acquired 2D GIWAXS data was visualized as colormap images using the jet color scheme. Sections showing the region of the (100) diffraction peak were extracted too (see Figure S1 as an example).

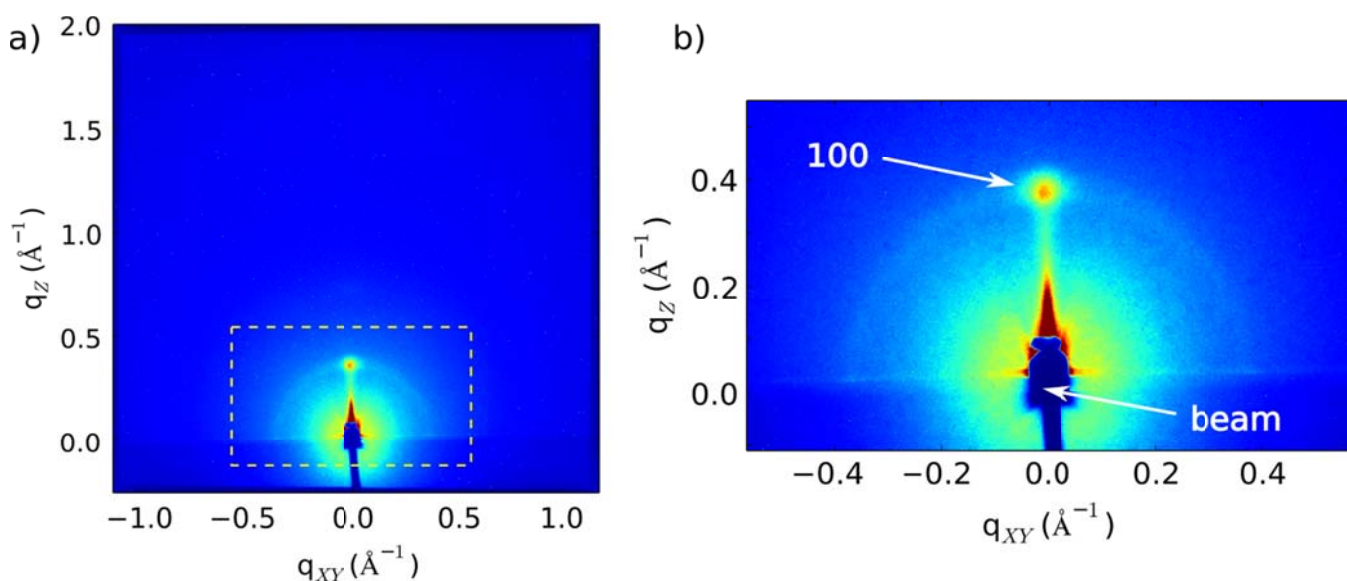


Figure S1. Example of the two-dimensional Grazing Incidence Wide Angle X-ray Scattering (GIWAXS) image of the P3HT sample, a) full image acquired, with the 100 section highlighted with a dashed line rectangle ; b) zoomed in section showing the 100 peak.

The z (out of plane) cross-sections of the 2D GIWAXS data were extracted and plotted as a dependence on scattering vector q. Subsequently, baseline was subtracted from all the plots and the (100) peaks were interpolated with Gaussian function. Where applicable, a sum of two Gaussians was used as a function to interpolate, leading to the deconvolution of the existing peaks into two separate (100) P3HT phases (see figure S2 and figures 1c), d) in the main text).

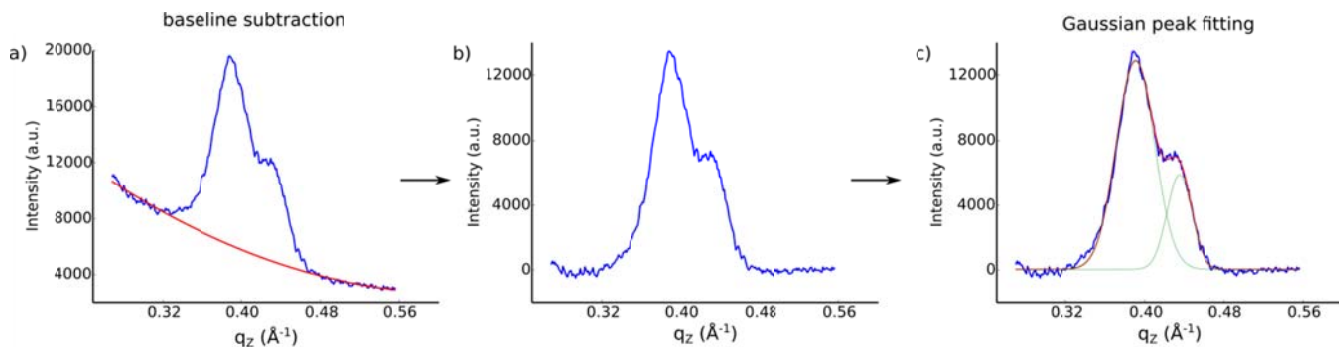


Figure S2. GIWAXS peak analysis procedure: a) baseline estimation (red line); b) baseline-corrected curve; c) Gaussian peak fitting of the curve.

The corresponding crystallographic parameters (d-spacing, coherence length L and peak intensities) were calculated. The d-spacing was calculated using the Bragg's equation, and Debye-Scherrer formula was used for the estimation of coherence length values. The peak intensities were calculated as the total area of the corresponding peak.

High M_n P3HT batch		
QBT (wt%)	p_1 intensity (counts)	p_2 intensity (counts)
0	6.15×10^5	-
0.3	5.83×10^5	1.77×10^5
0.6	5.32×10^5	1.60×10^5
1	7.97×10^5	0.63×10^5
Low M_n P3HT batch		
QBT (wt%)	p_1 intensity (counts)	p_2 intensity (counts)
0	7.59×10^5	4.38×10^5
0.3	6.86×10^5	2.51×10^5
0.6	4.92×10^5	2.06×10^5
1	5.41×10^5	3.33×10^5

Table S1. QBT composition dependent GIWAXS intensities of the non-densely packed P3HT (p_1) and the densely packed P3HT (p_2) polymorphs signals (see fitted GIWAXS data shown in Figures 1c,d and Table 1 in the main text) in the P3HT:PCBM:QBT ternary composites prepared by a high M_n and a low M_n rr-P3HT batch.

Atomic Force Microscopy (AFM) measurements

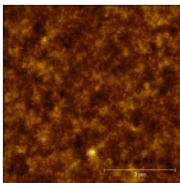
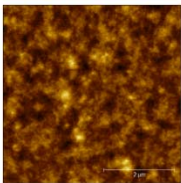
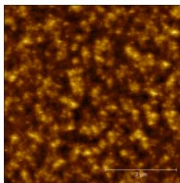
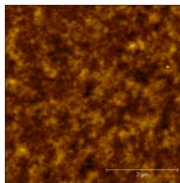
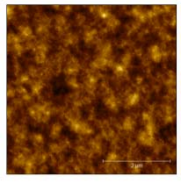
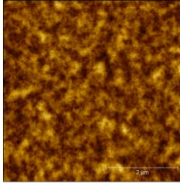
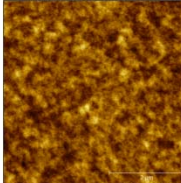
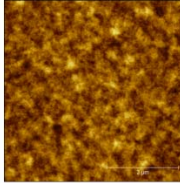
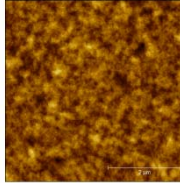
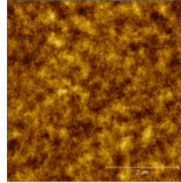
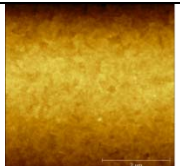
Sample	0 wt%QBT	0.3 wt% QBT	0.6 wt% QBT	1 wt% QBT	3 wt% QBT
High M_n rr-P3HT blend films					
Low M_n rr-P3HT blend films					
PEDOT:PSS only					

Table S2. Composition dependent tapping mode AFM images ($5 \mu\text{m} \times 5 \mu\text{m}$, topography) of P3HT:PCBM:QBT films prepared by high and low M_n batches of rr-P3HT. All films deposited onto glass/ITO/PEDOT:PSS layers. For comparison the AFM image of a PEDOT:PSS-only layer on glass/ITO substrate is also presented.

UV-Vis absorption characterization measurements

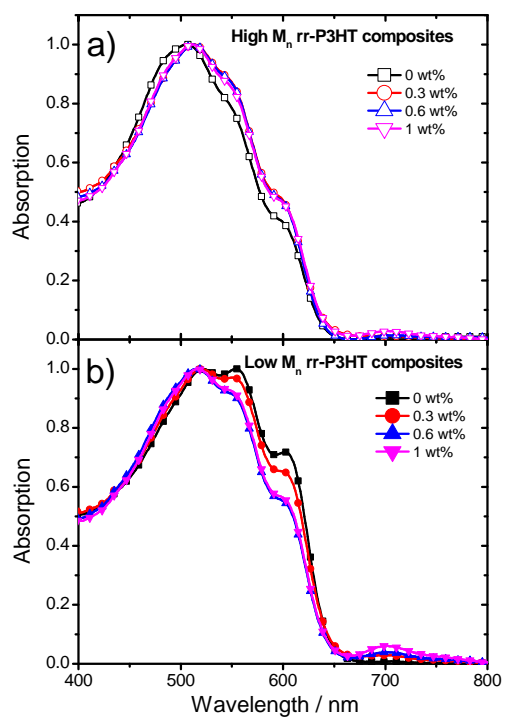


Figure S3. Composition dependent UV-Vis absorption spectra for thin films of P3HT:PCBM:QBT composites as prepared by the a) high- M_n P3HT derivative and b) low- M_n P3HT derivative, with QBT content of 0 wt% (squares), 0.3 wt% (circles), 0.6 wt% (up-triangles) and 1 wt% (down-triangles).

Space Charge Limited Current (SCLC) measurements

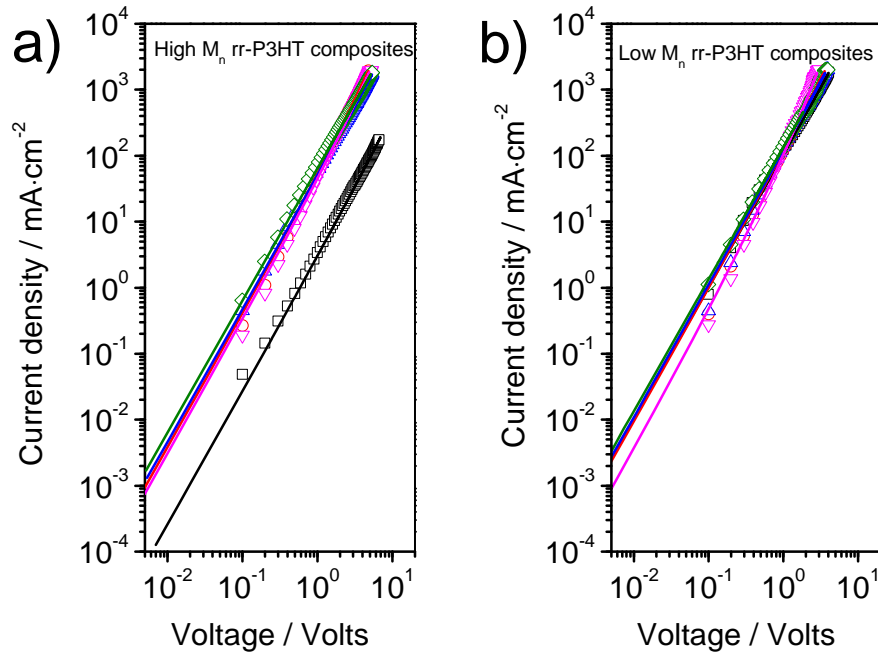


Figure S4. Dark J - V curves of P3HT:PCBM:QBT hole-only devices with photoactive layers prepared by the a) high M_n rr-P3HT batch and b) the low M_n rr-P3HT batch, with increasing QBT content: 0 wt% (squares), 0.3 wt% (circles), 0.6 wt% (up-triangles), 1 wt% (down-triangles) and 3 wt% (diamonds). In all cases the device structure was ITO/PEDOT: PSS/P3HT:PCBM:QBT/Au. The solid lines are fits to the data according to Equation (1).

The dark current density - voltage curves of each device was fitted according to a modified Mott-Gurney equation that takes into consideration the Poole-Frenkel effect:

$$J_{sclc} = \frac{9}{8} \epsilon_0 \epsilon_r \mu \frac{V^2}{L^3} \exp(0.89\beta \sqrt{\frac{V}{L}}) \quad (1)$$

In Equation 1 β is the electric field-activation factor of mobility and accounts for the degree of disorder, particularly the energetic level distribution of the carrier hopping sites in the material, i.e., a smaller β indicates a lower degree of energetic disorder. Also, ϵ_0 is the electric permittivity of free space, ϵ_r is the relative dielectric constant of the active layer, μ is the charge carrier mobility, L is the thickness of the device photoactive layer and V is the voltage applied on the device.

Transient photovoltage (TPV) measurements

Photodiodes with photoactive layers of P3HT:PCBM:QBT (device structure glass/PEDOT:PSS/P3HT:PCBM:QBT/Al) were directly connected to an Agilent 3000 oscilloscope with an input impedance of $1\text{M}\Omega$ and they were photoexcited with a 532 nm laser pulse of 10 ns pulse length and a 10 Hz repetition rate. TPV measurements were carried out under a constant background illumination of 1 Sun. Laser intensity and background illumination intensity were varied by a set of neutron density filters. The initial laser pulse energy was kept between $12.97\ \mu\text{J}$ to $15.96\ \mu\text{J}$.

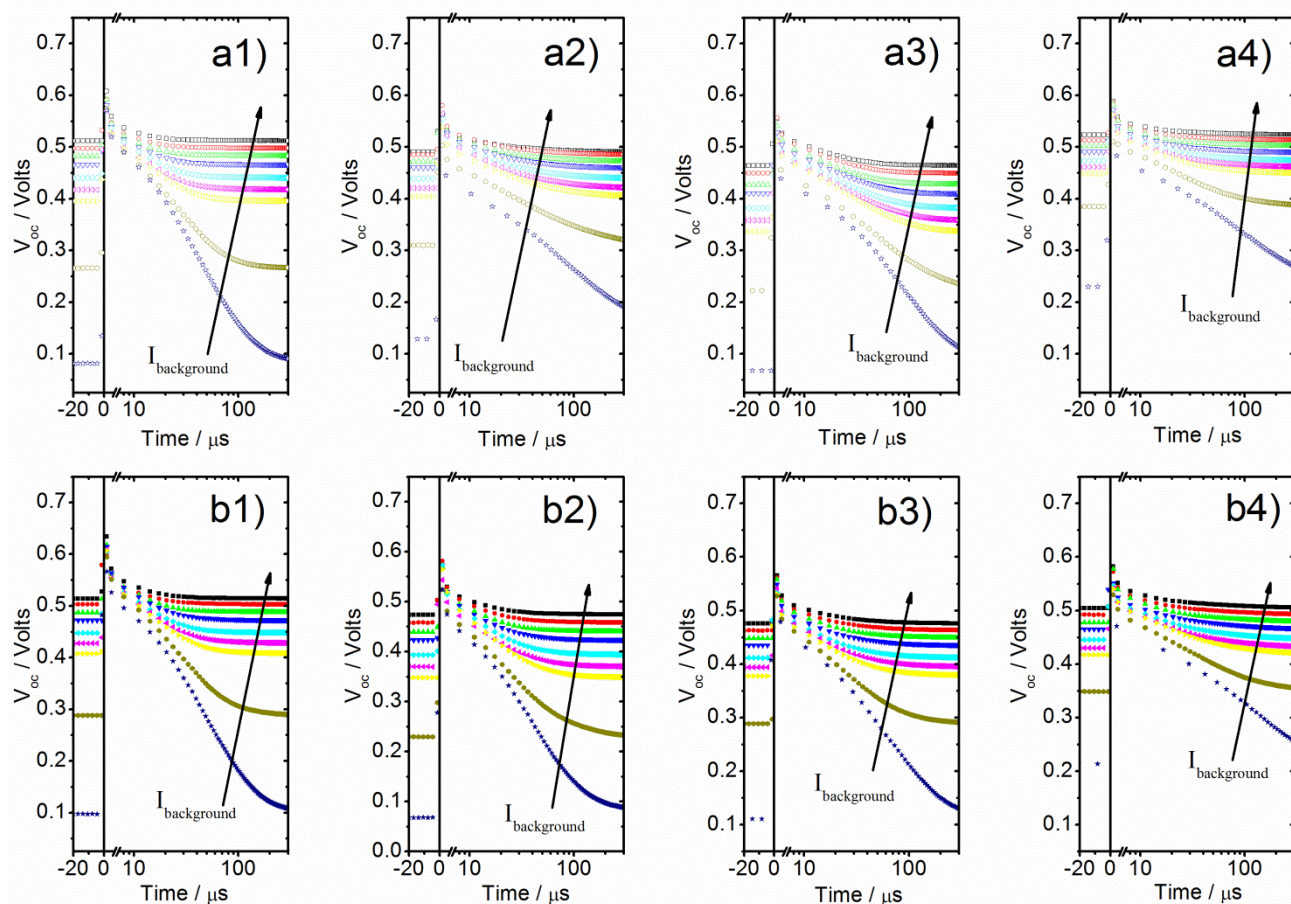


Figure S5. Light intensity dependent photovoltage transients of solar cell devices with P3HT:PCBM:QBT photoactive layers prepared by a) the high M_n P3HT batch (filled symbols) and b) the low M_n P3HT batch (open symbols) and with increasing QBT content: a1/b1) 0 wt%, a2/b2) 0.3 wt%, a3/b3) 0.6 wt%, and a4/b4) 1 wt%. The intensity of the white light background illumination ($I_{\text{background}}$) was progressively increased in the steps of $1.9\ \text{mWcm}^{-2}$, $13.2\ \text{mWcm}^{-2}$, $39.7\ \text{mWcm}^{-2}$, $50.0\ \text{mWcm}^{-2}$, $62.3\ \text{mWcm}^{-2}$, $88.3\ \text{mWcm}^{-2}$, $107.5\ \text{mWcm}^{-2}$, $130.3\ \text{mWcm}^{-2}$ and $160.0\ \text{mWcm}^{-2}$.

Differential Scanning Calorimetry (DSC) measurements

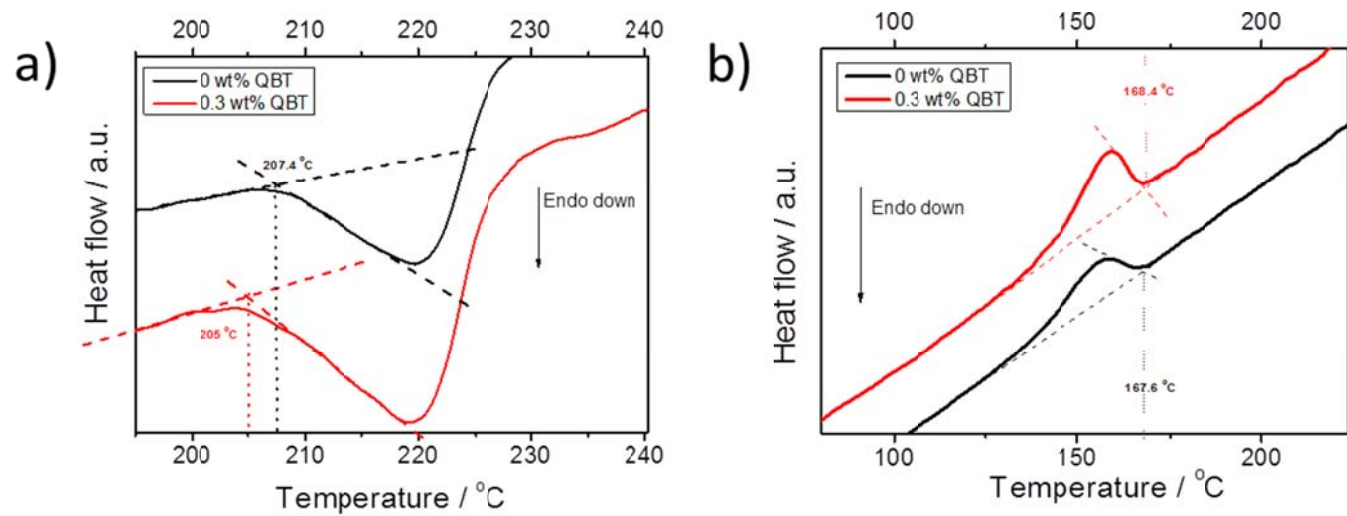


Figure S6. Differential scanning calorimetry thermograms of P3HT:PCBM:QBT ternary composites with QBT content of 0 wt% (black line) and 0.3 wt% (red line) as obtained for the a) heating scan and b) cooling scan of the samples. Further information on the details of the DSC measurements can be found in Reference [43] of the main text.